DOI: 10.1002/ejic.200600370

Synthesis and Some Properties of Bis(ruthenocenyl)thiophene Derivatives – Possible Spin-Coupling in the Two-Electron Oxidized Species of Dinuclear Ruthenocenes Bridged by Thiophene Derivatives

Masaru Sato,*[a] Yusuke Kubota,[a] Atsushi Tanemura,[a] Genta Maruyama,[a] Takashi Fujihara,[a] Juzo Nakayama,[a] Toshiyuki Takayanagi,[a] Kenta Takahashi,[a] and Kei Unoura[b]

Keywords: Metallocenes / Redox chemistry / Cations / Sulfur heterocycles / Oxidation / Metal–metal interactions

The binuclear ruthenocene derivatives bridged by thiophene, 3,4-ethylenedioxythiophene, 2,2′-bithiophene, thieno[3,2-*b*]thiophene, or 3,6-dimethylthieno[3,2-*b*]thiophene were prepared by the Suzuki coupling of 2-ruthenocenyl-4,5-tetramethyl-1,3-dioxaborolane with the corresponding diiodo compounds. In addition, thiophene- and bithiophene-bridged binuclear pentamethylruthenocenes were prepared by the reaction of bis(pentamethylruthenocenyl)diyne and -tetrayne with NaSH, respectively. The cyclic voltammograms of these complexes exhibit one-step two-electron redox waves in the lower potential region (0–0.3 V versus FcH/FcH^+). The two-electron oxidized species of the thiophene-bridged binuclear ruthenocene derivatives are comparatively stable and adopt the spin-coupled and structurally isomerized fulvene complex-type structure. The solid structure of the oxidized species of bis(pentamethylruthenocenyl)thiophene was determined by X-ray diffraction analysis. The thieno[3,2-*b*]thiophene-bridged analog shows a temperature-dependent ^1H NMR spectrum in CD_3NO_2. The dicationic species exist as a Ru^{II}–Ru^{IV} mixed-valence species in CD_3CN.

Introduction

Significant interest has been focused on carbon-rich organometallics that contain rigid, π-conjugated chains or aromatics because organometallic assemblies are important for electron-transfer processes,[1] the formation of liquid crystalline materials,[2] and the construction of molecular devices.[3] In particular, numerous investigations have been concentrated on polyynediyl complexes, $[L_nM–(C\equiv C)_m–ML_n]$ (m = 1,2, etc.),[4] because they are attractive candidates for use in the preparation of molecular wires and nanoscale electronic devices; this comes by virtue of their possible charge delocalization along the entire conjugated backbone.[5] Ferrocenyl derivatives also present themselves as fascinating candidates for use in the design of such materials because of a stable one-electron redox system (i.e. stability in both the neutral and oxidized forms).[6] Enormous effort has been expended in the synthesis of dinuclear ferrocene derivatives with π-conjugation.[7] In addition, much attention is currently focused on materials that are based on oligothiophenes and polythiophenes because of their remarkable electronic and optoelectronic properties.[8,9] Therefore, the incorporation of these compounds between two ferrocenyl sites may be expected to promote or inhibit electron delocalization in these types of conjugated systems.[10] Only a few studies have been published with regard to ruthenocene derivatives bridged by π-conjugated chains probably because of the irreversible redox behavior of ruthenocene itself. For example, biruthenocene undergoes one-step two-electron oxidation to afford the dicationic complex that possesses a uniquely coordinated fulvalene as a result of structural isomerization caused by spin-coupling.[11] Bis(ruthenocenyl)oligoenes are oxidized reversibly by the one-step two-electron redox process to afford stable dicationic bis(fulvene)-type complexes.[12] The spin coupling that leads to this structural isomerization is maintained despite the length of the conjugation, at least up to the tetraene derivatives. Bis(ruthenocenyl)ethynes also afford the novel dicationic μ_2-bis(cyclopentadienylidene)ethene diruthenium complexes upon two-electron oxidation.[13] In contrast with the case of the two-electron oxidized species of the oligoene derivatives, the stability of the two-electron oxidized species in the oligoyne derivatives declines with increasing length of the conjugation. In cyclic voltammograms, these dinuclear ruthenocene derivatives show two-electron oxidation waves in the low-potential region, which suggests the formation of a stable, two-electron oxidized

[a] Department of Chemistry, Faculty of Science, Saitama University,
Saitama, Saitama 338-8570, Japan
[b] Department of Chemistry, Faculty of Science, Yamagata University,
Yamagata, Yamagata 990-8560, Japan

species. However, the bis(ruthenocenyl) derivatives that are bridged by benzenoid aromatics show only a small or no two-electron oxidation wave in their cyclic voltammograms.[14] The published reports on the ferrocenes and transition-metal complexes bridged by thiophene derivatives[9,10] have stimulated us to investigate complexes that incorporate thiophene derivatives between two ruthenocenyl sites because thiophenes have an enhanced olefinic character and have less aromaticity compared with those of benzenoid compounds. In this report, we describe the synthesis and some properties of bis(ruthenocenyl)thiophene derivatives. Recently, a bis(ruthenocenyl)thiophene derivative has been reported to show an interesting redox behavior.[15]

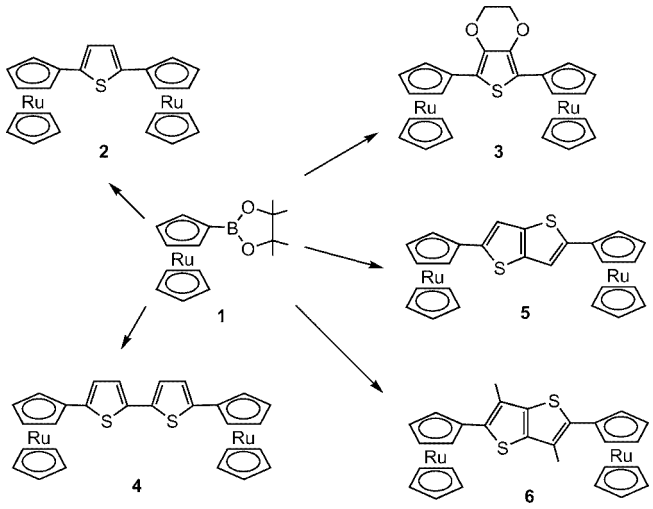

Scheme 1.

Results and Discussion

Preparation of Bis(ruthenocenyl)thiophene Derivatives

It has been reported that the Suzuki coupling reaction of 2-ruthenocenyl-4,5-tetramethyl-1,3-dioxaborolane (**1**) with the appropriate halide is a useful method for the preparation of binuclear ruthenocene derivatives bridged by an aromatic compound.[14] Complex **1** was heated with 2,5-diiodothiophene in the presence of (dppf)$PdCl_2$ and 3 M aqueous NaOH in DME in a sealed tube to afford 2,5-bis(ruthenocenyl)thiophene (**2**) in 23% yield. In a similar manner, the reaction of **1** with 3,4-ethylenedioxy-2,5-diiodothiophene, 5,5′-diiodo-2,2′-bithiophene, 2,5-diiodothieno[3,2-*b*]thiophene, or 2,5-diiodo-3,6-dimethylthieno[3,2-*b*]thiophene also proceeded successfully under the similar conditions to afford the corresponding binuclear ruthenocene derivatives **3**, **4**, **5**, or **6** with yields of 33%, 23%, 18%, or 25%, respectively (Scheme 1). Complex **2** was also prepared by the reaction of 1,4-bis(ruthenocenyl)buta-1,3-diyne with NaSH in DMF in an 87% yield. Complexes **2**, **4**, and **5** were scarcely soluble in common organic solvents. Assignment of their structures was carried out on the basis of the corresponding spectroscopic data. For example, the ^{1}H NMR spectrum of **4** shows the η-C_5H_4-ring protons at δ = 4.63 and 4.98 ppm as triplets (J = 1.8 Hz), the η-C_5H_5-ring protons at δ = 4.53 ppm as a singlet, and the ring protons of bithiophene at δ = 6.82 and 6.86 ppm as doublets (J = 3.8 Hz). The ^{13}C NMR spectrum of **4** supports the structure assigned by the ^{1}H NMR spectrum. The structure of **3** was confirmed by single-crystal X-ray diffraction. The crystallographic data are listed in Table 5, and selected bond lengths and angles are listed in Table 1. The ORTEP view of **3** is shown in Figure 1. The two η-C_5H_4-ring planes of the ruthenocenyl (abbreviated as Rc hereafter) parts are tilted by 18.89(4)° and 24.83(4)° toward the central thiophene-ring plane probably because of the steric hindrance that is due to the dioxolane ring fused to the thiophene ring. The two η-C_5H_5Ru moieties of the Rc parts are positioned on opposite sides of the central thiophene ring. Other bond lengths and angles are the same as those of the ruthenocene and thiophene derivatives.

Table 1. Selected bond lengths and bond angles for **3**.

Bond lengths [Å]			
C(11)–C(12)	1.380(11)	C(12)–C(15)	1.400(11)
C(15)–C(16)	1.367(11)	C(12)–O(1)	1.378(9)
O(1)–C(13)	1.38(2)	C(13)–C(14)	1.31(2)
C(14)–O(2)	1.432(14)	O(2)–C(15)	1.366(10)
S(1)–C(11)	1.742(9)	S(1)–C(16)	1.735(8)
C(1)–C(11)	1.413(12)	C(16)–C(17)	1.425(12)
Ru(1)–C(Cp)	2.176(av.)	C(Cp)-C(Cp)	1.42(av.)
Bond angles [°]			
C(11)–S(1)–C(16)	94.4(4)	S(1)–C(11)–C(12)	107.1(6)
C(11)–C(12)–C(15)	115.7(7)	S(1)–C(16)–C(15)	108.9(6)
C(12)–C(15)–C(16)	113.8(7)		

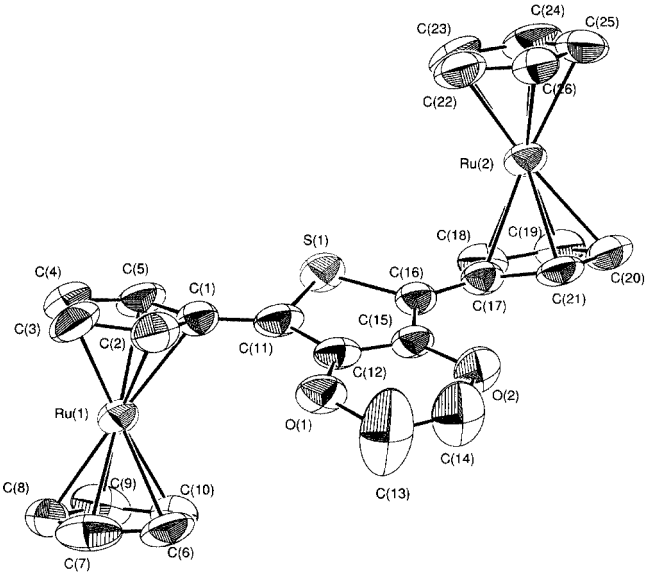

Figure 1. ORTEP view of complex **3**.

1,4-Bis(1′′,2′′,3′′,4′′,5′′-pentamethylruthenocenyl)buta-1,3-diyne was allowed to react with NaSH in DMF heated at 100 °C under an argon atmosphere to afford 2,5-bis(1′′,2′′,3′′,4′′,5′′-pentamethylruthenocenyl)thiophene (**7**) in 92% yield. The similar reaction of 1,8-bis-(1′′,2′′,3′′,4′′,5′′-pentamethylruthenocenyl)-1,3,5,7-octatetrayne afforded 5,5′-bis(1′′,2′′,3′′,4′′,5′′-pentamethylruthenocenyl)-2,2′-bithiophene (**8**) in 64% yield (Scheme 2). The structures of these compounds were assigned on the basis of the corresponding ^{1}H- and ^{13}C NMR spectroscopic data. The structure of **7** was also confirmed by X-ray diffraction analysis. The crystallographic data are listed in Table 5, and selected bond lengths and angles are shown in Table 2. The ORTEP view of **7** is shown in Figure 2. The thiophene ring is almost coplanar with the plane of the η-C_5H_4-rings of the two 1′,2′,3′,4′,5′-pentamethylruthenocenyl (abbreviated as Rc* hereafter) groups; the twisted angles are 3.60(5)° and 2.36(5)°. The two η-C_5Me_5Ru moieties of the Rc* parts adopt the *trans* orientation with respect to the linker ligand. Other bond lengths and angles are the same as the corresponding parameters for the ruthenocene and thiophene derivatives.

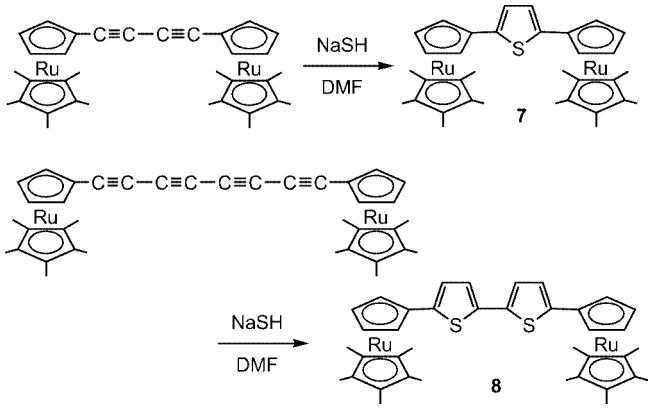

Scheme 2.

Table 2. Selected bond lengths and bond angles for **7**.

Bond lengths [Å]			
Ru(1)–C(Cp) av.	2.187	C–C(Cp) av.	1.42
S(1)–C(1)	1.736(9)	S(1)–C(4)	1.748(8)
C(1)–C(2)	1.352 (13)	C(2)–C(3)	1.390(12)
C(3)–C(4)	1.336 (12)	C(1)–C(20)	1.445(11)
C(4)–C(5)	1.443(12)		
Bond angles [°]			
S(1)–C(1)–C(2)	109.0(7)	S(1)–C(4)–C(3)	109.0(7)
S(1)–C(4)–C(5)	120.3(6)	S(1)–C(1)–C(20)	121.1(7)
C(1)–C(2)–C(3)	114.1(13)	C(2)–C(3)–C(4)	115.0(8)
C(1)–S(1)–C(4)	92.5(4)		

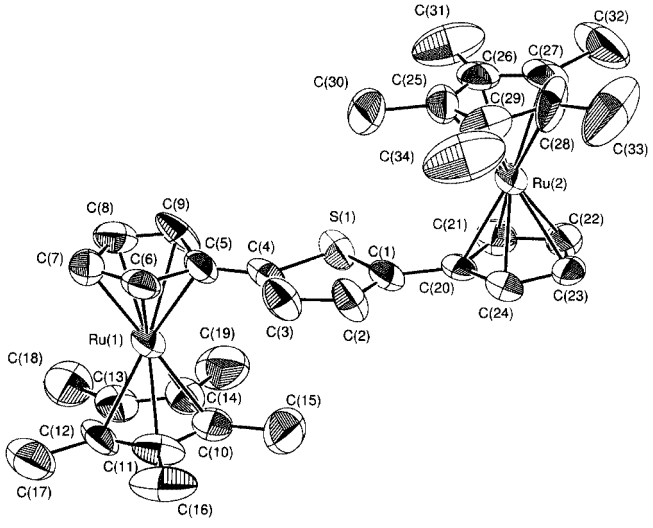

Figure 2. ORTEP view of complex **7**.

Redox Behavior

The cyclic voltammograms of **2**–**8** were measured in a solution of 0.1 M nBu$_4$NBF$_4$ in CH_2Cl_2 with the use of a glassy carbon electrode and a sweep rate of 0.1 V s^{-1} (Figure 3). The electrochemical data are summarized in Table 3. As seen in Figure 3, the cyclic voltammograms are much more complex than those of bis(ruthenocenyl)ethenes that were previously reported to contain a pair of oxidation and reduction waves in a similar region.[12] However, the cyclic voltammograms exhibit a definite oxidation wave near 0.3 V, along with a similar wave near 0.5 V in the Rc series **2**–**6**. The magnitude of the former oxidation wave is almost equal to that of the latter, probably because the electron-rich thiophene bridge promotes the one-step two-electron redox process. This observation differs greatly from the finding that similar dinuclear ruthenocene derivatives bridged by aromatics only show a small or no oxidation wave near 0.3 V.[14] In these complexes, the peak current parameter I_{pa} at about 0.3 V is about 2500 μAV$^{-1/2}$s$^{1/2}$ cm^{-2}mM^{-1}, with the exception of **4**, and the n_{app} value in the thin-layer coulometry[16] is approximately 2; this suggests that the first oxidation wave near 0.3 V can be assigned to the two-electron oxidation process that corresponds to the Ru^{II}–Ru^{III} couple at the two ruthenocenyl sites. The large peak current parameter for the first oxidation peak of **4** appears to be due to an overlap of the first oxidation peak with part of an adjacent, second oxidation peak. Although the redox behavior of the second wave of each complex is relatively complex, the second wave near 0.5 V may be assigned to Ru^{III}–Ru^{IV} oxidation. Moreover, if the backwards scan is analyzed at the end of the first wave near 0.3 V, the I_{pa} of this oxidation wave is almost identical to the I_{pc} of the reduction wave near 0.2 V. Surprisingly, in **7** and **8** one oxidation wave and one reduction wave appear near 0.0 V with equal magnitudes, although small additional peaks are also observed. The methyl-substituted ruthenocene ring seems to assist the one-step two-electron redox process. In particular, the oxidation potential of **7** is in the low potential region, which is similar to those of bis(ruthenocenyl)-ethenes (which are comparable to that of ferrocene!).[12] These observations suggest that the redox waves observed at <0.25 V correspond to a one-step two-electron process and that the two-electron oxidized species of complexes **2**–**8** are stable.

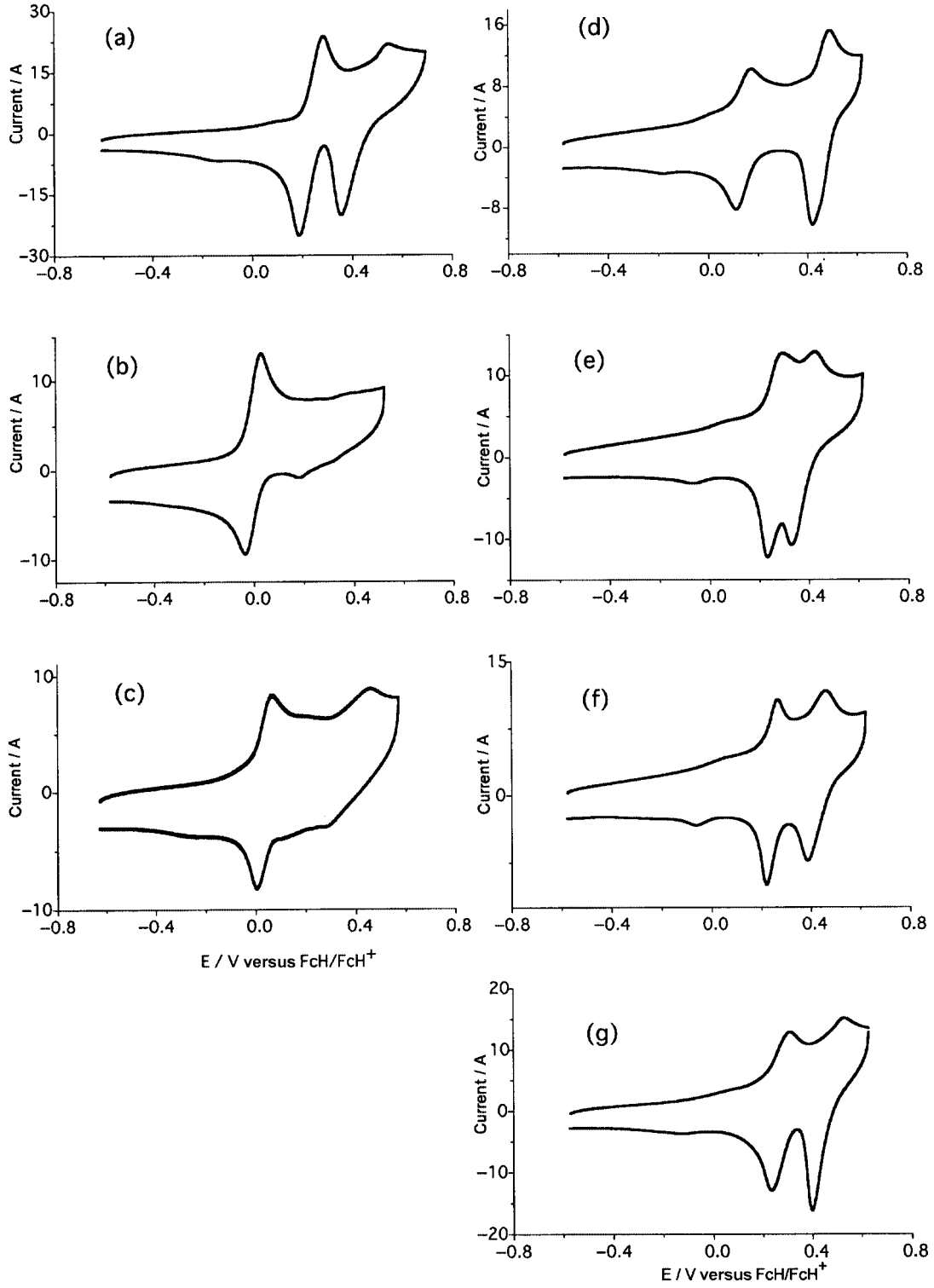

Figure 3. Cyclic voltammograms of **2**–**8**: (a) complex **2**, (b) complex **7**, (c) complex **8**, (d) complex **3**, (e) complex **4**, (f) complex **5**, (g) complex **6**.

It is noteworthy that the oxidation potentials observed for the present complexes show no change or increased only slightly with increases in conjugation of the linker: **2** (+0.281 V) ≈ **5** (+0.265 V) ≈ **4** (+0.276 V), and **7** (+0.028 V) < **8** (+0.069 V). A similar but clearer trend is observed in the Rc*(C≡C)$_n$Rc* series.[13a] However, this tendency is different from that observed for the dinuclear ruthenocene derivatives bridged by oligoenes, the oxidation potentials of which are shifted to a lower potential region with an increase in the number of CH=CH units.[12a] The lower susceptibility of the oxidation potential to the length of conjugation in the present system seems to be related to

Table 3. Cyclic voltammetric[a] and coulometric data for the first oxidation process of bis(ruthenocenyl)thiophene derivatives in CH_2Cl_2.

Complex	E_{pa} [V] vs. FcH/FcH^+	E_{pc} [V] vs. FcH/FcH^+	$E_{1/2}$ [V][b] vs. FcH/FcH^+	ΔE_p [mV][c]	I_{pa} [U][d]	I_{pc}/I_{pa}	n_{app}[e]
2	0.281	0.201	0.241	80	2900	1.1	2.2(1)
3	0.174	0.111	0.143	63	2500	1.2	1.9(1)
4	0.276	0.229	0.253	47	4400	1.6	–[f]
5	0.265	0.224	0.245	41	3000	1.4	–[g]
6	0.307	0.230	0.269	77	2400	1.5	1.8(1)
7	0.028	–0.039	–0.005	67	2700	1.0	2.1(2)
8	0.069	0.007	0.038	62	2700	1.3	–[g]

[a] Sweep rate = 0.1 Vs^{-1}. [b] $E_{1/2} = (E_{pa} + E_{pc})/2$. [c] $\Delta E = E_{pa} - E_{pc}$. [d] Peak current parameter: $U = \mu A V^{-1/2} s^{1/2} cm^{-2} mM^{-1}$. [e] The number of electrons (n_{app}) concerned with the first oxidation of the complexes with standard deviation given in parentheses is determined from the results of thin-layer coulometry. [f] The second oxidation is observed at the potential close to the first oxidation. [g] Solubility is too low to determine n_{app}.

the fact that the aromaticity of the thiophene ring works as cross-conjugation for the electronic interaction between two metal sites in the bis(ruthenocenyl)thiophene derivatives.

Chemical Oxidation

A suspension of thiophene-bridged dinuclear ruthenocene **2** in $CHCl_3$ was oxidized with *p*-BQ/BF_3·OEt_2 (*p*-BQ = *p*-benzoquinone) at 0 °C to yield **9** as fine brown crystals. The deep red–brown solution of **9** in CD_3NO_2 was found to be stable at 0 °C. The ^1H NMR spectrum shows one singlet for the η-C_5H_5 ring protons at δ = 5.26 ppm, the four signals for the η-C_5H_4 ring protons at δ = 5.75, 5.90, 6.32, and 6.40 (2 H each) ppm, and one singlet for the thiophene ring protons at δ = 7.46 ppm, which suggest that the molecule has a mirror plane or a center of symmetry but that the α- and β-protons of the η-C_5H_4 ring are nonequivalent because of the lack of symmetry in the η-C_5H_4 ring. The η-C_5H_5 ring ($\Delta\delta$ = 1.61 ppm) and the thiophene ring protons ($\Delta\delta$ = 0.77 ppm) are shifted to a lower field compared with the corresponding signals of **2**, which indicates the accumulation of positive charges on the Rc moiety and the thiophene ring. This type of spectral pattern accords with the appearance of the fulvene complex-type structure (**9B** in Scheme 3), as seen for the oxidized species of bis(ruthenocenyl)ethene.[12] This hypothesis is supported by the ^{13}C NMR spectrum of **9** in which signals for the α- and β-η-C_5H_4 ring carbons are observed at δ = 77.42, 78.72, 90.33, and 90.66 ppm. This signal pattern is also observed for [(η-C_5H_5)Ru(μ$_2$-η^6:η^6-$C_5H_4CHCHC_5H_4$)Ru(η-C_5H_5)]-$(BF_4)_2$.[12]

Oxidation of **7** with *p*-BQ/BF_3OEt_2 in CH_2Cl_2 at 0 °C and subsequent dilution with benzene produced **11** as black powdery crystals that are stable when stored in the freezer. The ^1H NMR spectrum of the red–violet solution of **11** in CD_3NO_2 at –5 °C exhibits the η-C_5H_4 ring proton signals at δ = 5.53 (m, 4 H) and 5.90 (m, 4 H) ppm and the thiophene ring proton signals at δ = 7.41 ppm. This signal pattern is different from that observed for **9**, which implies that the α- and β-protons of the η-C_5H_4 ring are in a symmetrical environment. The signals for the η-C_5H_4 ($\Delta\delta$ = 1.30 and 1.33 ppm) and thiophene ring ($\Delta\delta$ = 0.75 ppm) protons in **12** show a lower-field shift similar to those seen for **9**. Therefore, the spectral pattern indicates the presence of species **11A** shown in Scheme 3, in which the two spins of the molecule are coupled to each other, but they do not lead to structural isomerization. However, the ^{13}C NMR spectrum of **11** in CD_3NO_2 shows four η-C_5H_4 ring carbon signals at δ = 75.85, 77.10, 93.81, and 93.99 ppm. This signal pattern is similar to that seen for **9**, which indicates the presence of a fulvene complex-type structure (**11B**) for the dicationic species. The appearance of two signals for the η-C_5H_4 ring protons in the ^1H NMR spectrum of **11** in CD_3NO_2 may be due to an accidental superimposition because the signals are observed as a quintet and a sextet rather than two triplets, if they are examined in detail. Furthermore, in CD_2Cl_2 or $(CD_3)_2CO$ three signals are observed for the η-C_5H_4 ring protons.

The NMR spectra of **9** and **11** in CD_3CN show quite different patterns from those in CD_3NO_2, and two sets of the signals for the Rc part and the thiophene ring are observed. For example, the set of signals for the Rc ring protons [δ = 4.57 (s, 5 H), 5.02 (t, 2 H), and 5.36 (t, 2 H) ppm] is similar to that of the neutral ruthenocenyl group, and the other set of signals [δ = 5.90 (s, 5 H), 6.01 (t, 2 H), 6.27 (t, 2 H) ppm] resembles that of the ruthenocenium cation. The protons of the thiophene ring appear at δ = 7.40 and 8.05 ppm as doublets (J = 4.5 Hz). The spectral pattern indicates that **9** reacts with CD_3CN, passes through intermediate **9C**, to generate Ru^{II}–Ru^{IV} mixed-valence complex **10**. Similarly, the ^1H NMR spectrum of **11** in CD_3CN shows the presence of mixed-valence complex **12**. This type of conversion has been reported for the dissolution of the two-electron oxidized species of biruthenocene in CD_3CN,[11] but has not been observed for the oxidized species of the dinuclear ruthenocenes bridged by oligoenes and oligoynes in CD_3CN.[12,13] This difference may be due to the level of stability of the fulvene complex-type structure. It is considered that the two-electron oxidized species of bis(ruthenocenyl)oligoenes are sufficiently stabilized by the fulvene complex-type structure, whereas the fulvene complex-type structure in **9** or **11** is not very stable in solution because of lower spin coupling. These results also suggest that the replacement of the Rc group with the Rc* group exerts little influence on the structures of the two-electron oxidized species of the thiophene-bridged binuclear derivatives.

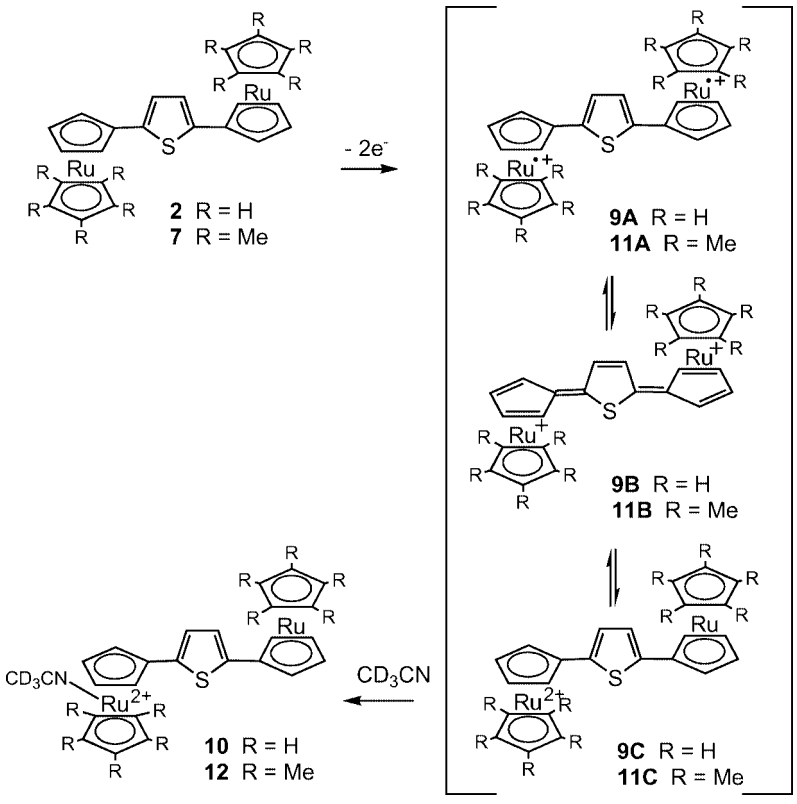

Scheme 3.

The oxidation of **7** with ferricenium tetra[3,5-bis(trifluoromethyl)phenyl]borate in CH_2Cl_2 yielded stable oxidized species **13** as dark violet fine needles. The ^1H NMR spectrum of **13** in CD_3NO_2 exhibits two C_5H_4-ring protons at δ = 5.52 (m, 4 H) and δ = 5.90 (m, 4 H) ppm and shows no change when **13** is cooled to –30 °C (CH_3NO_2, m.p. –29 °C). This spectral pattern is similar to that observed for **11**, which suggests that the counter anion has no influence on the degree of structural isomerization. Complex **13** was recrystallized from CH_2Cl_2/diethyl ether in diffusion mode to produce black–violet cubes, which were suitable for X-ray diffraction analysis. The crystallographic data for **13** are listed in Table 5, and selected bond lengths and angles are shown in Table 4. The ORTEP view for the cationic part of **13** is shown in Figure 4. The cationic molecule of **13** is located at an inversion center. Two molecules of diethyl ether are involved in the crystal. As seen in Figure 4, a disorder exists in the central thiophene ring of **13**. It is clear that the Rc* part of **13** adopts a fulvene complex-type structure. The Ru(1)–C(16) bond length is 2.111(5) Å, which is somewhat shorter than the corresponding bond lengths observed in $[Ru(\eta\text{-}C_5H_5)(\eta^6\text{-}C_5H_4CH_2)]^+$ [2.272(4) Å],[17] $[(\eta\text{-}C_5Me_5)Ru(\eta^6{:}\eta^6\text{-}C_5H_4CHCHC_5H_4)Ru(\eta\text{-}C_5Me_5)^{2+}$ [2.410 Å],[12] and $[(\eta\text{-}C_5Me_5)Ru(\eta^6{:}\eta^6\text{-}C_5H_4C{=}CC_5H_4)Ru(\eta\text{-}C_5Me_5)^{2+}$ [2.254(3) Å].[13] The C(15)–C(16) bond length is 1.381(7) Å, which is shorter than the $C(sp^2)$–$C(sp^2)$ bond length (1.465 Å). Similar short bond lengths are found in the fulvene complexes $[Ru(\eta\text{-}C_5Me_5)(\eta^6\text{-}C_5Me_4CH_2)]^+$ [1.401(4) Å][18] and $[Ru(\eta\text{-}C_5H_5)(\eta^6\text{-}C_5H_4CH_2)]^+$ [1.405(5) Å].[17] The C(15)–C(16) bond is folded by 30.5° from the $\eta\text{-}C_5H_4$ ring plane. This tilt angle is smaller than those of $[Ru(\eta\text{-}C_5H_5)(\eta^6\text{-}C_5H_4CH_2)]^+$ (42.6°),[17] $[Ru(\eta\text{-}C_5Me_5)(\eta^6\text{-}C_5Me_4CH_2)]^+$ (40.3°),[19] $[(\eta\text{-}C_5Me_5)Ru(\eta^6{:}\eta^6\text{-}C_5H_4CHCHC_5H_4)Ru(\eta\text{-}C_5Me_5)]^{2+}$ (40.4°)[12] and $[(\eta\text{-}C_5Me_5)Ru(\eta^6{:}\eta^6\text{-}C_5H_4C{=}CC_5H_4)Ru(\eta\text{-}C_5Me_5)]^{2+}$ (41.3°),[13b] but close to that of $[(\eta\text{-}C_5H_5)Ru(\eta^6{:}\eta^6\text{-}C_5Me_4C{=}CC_5Me_4)Ru(\eta\text{-}C_5H_5)]^{2+}$ (32.7°).[13a] In addition, some bond alternation is observed in the $\eta\text{-}C_5H_4$ ring of the Rc* moiety. The C(16)–C(17) and C(17)–C(18) bond lengths are 1.753(13) and 1.306(14) Å, respectively, which indicates that the former is a single bond and the latter is a double bond, although these measurements are not precise because of the presence of disorder in the system. This relationship is reverse to that noted for neutral thiophene deriv-

Table 4. Selected bond lengths and bond angles for **13**.

Bond lengths [Å]			
Ru(1)–C(Cp) av.	2.182	C–C(Cp) av.	1.397
S(1)–C(16)	1.560(8)	S(1)–C(16′)	1.539(8)
C(16)–C(17)	1.735(13)	C(17)–C(18)	1.306(14)
C(16′)–C(18)	1.754(13)	C(15)–C(16)	1.381(7)
C(11)–C(15)	1.439(9)	C(11)–C(12)	1.405(16)
C(12)–C(13)	1.346(19)	C(13)–C(14)	1.357(14)
C(14)–C(15)	1.439(9)	Ru(1)–C(16)	2.111(5)
Bond angles [°]			
S(1)–C(16)–C(17)	105.6(5)	S(1)–C(16′)-C(18)	105.7(5)
S(1)–C(16)–C(15)	141.8(7)	S(1)–C(16′)-C(15′)	143.6(7)
C(16)–C(17)–C(18)	110.5(9)	C(17)–C(18)–C(16′)	109.9(9)
C(15′)–C(16′)–C(18)	109.3(7)	C(16)–S(1)–C(16′)	108.2(3)

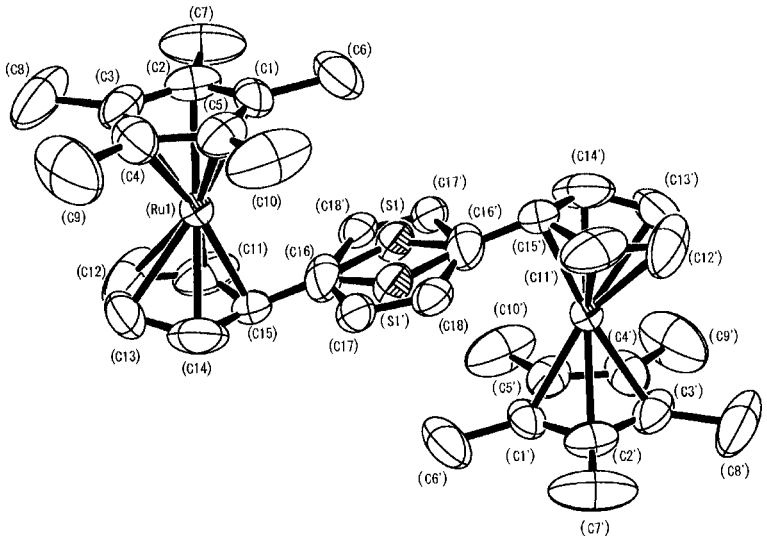

Figure 4. ORTEP view of complex **13**.

ative **7**. Therefore, the bridging ligand in **13** can be formulated as a fully conjugated 2,5-bis(fulvalenylidene)thiophene.

3,4-Ethylenedioxythiophene derivative **3** and bithiophene derivatives **4** and **8** were oxidized under similar conditions to generate the corresponding oxidized species, which gave no clear-cut ^{1}H NMR spectrum of a sole product in CD_3NO_2. Oxidation of thieno[3,2-*b*]thiophene derivative **5** under similar conditions afforded two-electron oxidized species **14** as a black powder which is relatively stable at room temperature in the solid form. The ^{1}H NMR spectrum of **14** in CD_3NO_2 at 20 °C shows η-C_5H_4 ring protons as triplets at δ = 5.93 and 6.30 ppm, which suggests that the structure of **14** has a plane or center of symmetry. The signals for the η-C_5H_4 ring protons broaden when the temperature is lowered, and the signal at δ = 5.93 ppm splits at –30 °C and is clearly observed as two signals at –35 °C (the limit of the measurement). This suggests the presence of a certain dynamic process. The structures **14A**–**14C** shown in Scheme 4 can be attributed to the structure of the two-electron oxidized species **14** in CD_3NO_2. The structure at low temperature that produces the four signals for the η-C_5H_4 ring protons (albeit two signals were still superimposed) seems to be fulvene complex-type structure **14B**. Thus, the structure at room temperature would be symmetrical structure **14A** or **14C**. The low-field shifts of the proton signals of η-C_5H_5 ($\Delta\delta$ = 0.74 ppm), η-C_5H_4 ($\Delta\delta$ = 1.25–1.30 ppm), and the thieno[3,2-*b*]thiophene rings ($\Delta\delta$ = 0.52 ppm) upon oxidation of **5** are smaller than those seen for **9**. The small shifts observed for the η-C_5H_5 and η-C_5H_4 ring protons suggest a decrease in the positive charge on the Ru atom of **14**. The lower-field shift of the thieno[3,2-*b*]thiophene ring protons may be explained by a counterbalancing of the increase in the positive charge by the destruction of the aromaticity in the thiophene ring of **14C**. Thus, **14C** seems to be the preferred structure at room temperature, and the dynamic process described above may be attributed to simultaneous charge transfer between **14B** and **14C**. However, a dynamic process due to spin-coupling and spin uncoupling between **14B** and **14A** cannot presently be ruled out. On the other hand, the ^{1}H NMR spectrum of **14** in CD_3CN shows two sets of signals for the (η-C_5H_5)Ru(η-C_5H_4)-moiety and two signals for the thieno[3,2-*b*]thiophene ring as observed for **10** and **12** in CD_3CN, which indicates that **15** reacts with CD_3CN via **14C** to generate Ru^{II}–Ru^{IV} mixed-valence complex **15**.

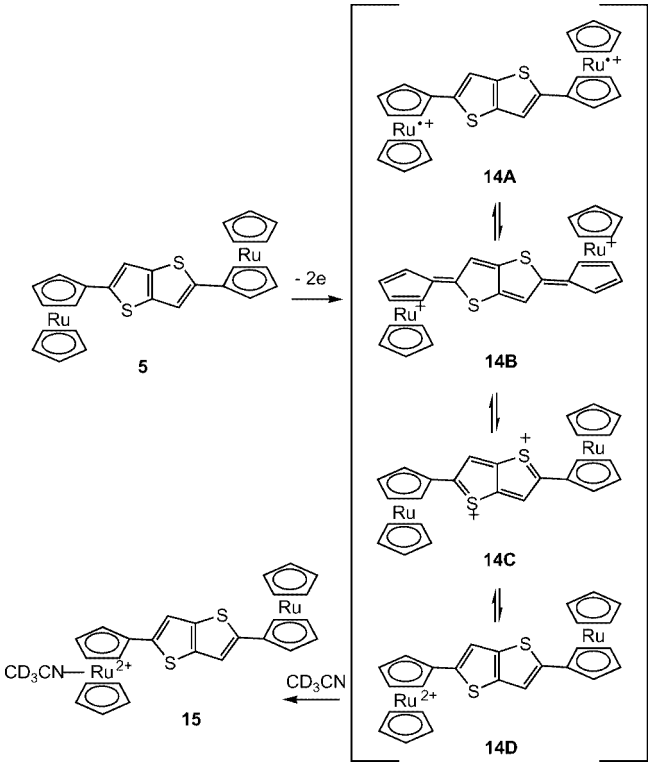

Scheme 4.

Theoretical Considerations

Density function theory (DFT) calculations were performed for the cationic part of two-electron oxidized species **9**, **11**, and **14**. Because the B3LYP/3-21G level calculation for the optimized structures of **9** and **11** did not reproduce the structures determined by the NMR spectra and X-ray diffraction analyses, local spin density approximation (LSDA) was employed for all calculations described in this paper, and in result could revive the actual structure.

The Rc* part of the two-electron oxidized species of thiophene-bridged complex **11** was found to adopt a fulvene complex-type structure, as shown in Figure 5. Thus, the Ru(1)–C(16) distance was found to be 2.50 Å, which is close to that found experimentally for **13** [2.529(5) Å]. The C(15)–C(16) bond length was calculated to be 1.412 Å, which is similar to that of the coordinated ethene bond and approximates the observed length [1.381(7) Å]. The C(15)–C(16) bond was found to be folded by 31.0° from the η-C_5H_4 ring plane, which is consistent with the experimental finding that the tilt angle in **13** is 30.5°, although this angle is smaller than those seen for fulvene complexes [Ru(η-C_5H_5)(η^6-$C_5H_4CH_2$)]$^+$ (42.6°)[17] and [Ru(η-C_5Me_5)(η^6-$C_5Me_4CH_2$)]$^+$ (40.3°).[18] The calculated C(16)–C(17) bond length (1.431 Å) resembles a single bond and the C(17)–C(18) bond length (1.354 Å) resembles a double bond, which coincides with the trend observed in **13**. The Mulliken charge distribution in two-electron oxidized species **11** was calculated, in which +0.929 of the positive charge was found to be located on one Ru atom and +0.001 of the positive charge was found to be located on the S atom. These results suggest that the structure of **11B** is that of the two-electron oxidized species **11**.

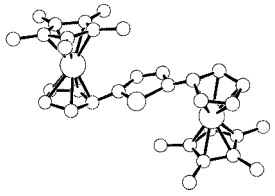

Figure 5. Optimized structure of the dication of **2**.

The optimized structure for the two-electron oxidized species of thieno[3,2-*b*]thiophene-bridged complex **14** was calculated to be also a fulvene complex-type structure (i.e. **14B**). This structure was experimentally detected at low temperature, although it was inconsistent with the structure at room temperature (vide supra). The calculation of the Mulliken charge distribution of **14** assigns a positive charge of about +0.3 on the sulfur atom, which suggests some contribution from **14C**. It was calculated that the conformer that possesses the thiophene ring perpendicular to the η-C_5H_4 ring, which explains the ^{1}H NMR spectrum at room temperature, has 125 kJ mol^{-1} more energy than the fulvene complex-type structure. In addition, calculations that considered both "broken-symmetry" and higher spin states were carried out. As a result, it was confirmed that the singlet states are electronic ground states in all cases and that the positive charge is equally distributed in the two terminal ruthenocene moieties. However, the lowest triplet states lie only about 40 kJ mol^{-1} higher in energy above the singlet ground states at the DFT levels of theory employed, and the optimized structures of the lowest triplet states have no fulvene complex-type structure. As one possible idea, the triplet state may be the ground state for **14** in solution, but there is no evidence to support this assumption at present. More systematic calculations that include solvent effects will be necessary, but this is beyond the scope of this paper.

Summary

The binuclear ruthenocene derivatives bridged by thiophene derivatives were newly prepared. The cyclic voltammograms for these complexes exhibited the one-step two-electron redox waves in a lower potential region, contrary to those for derivatives bridged by benzenoid aromatics.[11] This finding is probably related to increases in the electron-rich and olefinic properties of the thiophene derivatives. The stability levels and structures of the two-electron oxidized species were found to be mainly dependent on the types of bridging thiophene derivatives. The two-electron oxidized species of **3**, **4**, and **8** are unstable, whereas those of **2**, **5**, and **7** are stable. The two-electron oxidized species of **2** and **7** adopt the spin-coupled and structurally isomerized fulvene complex-type structures **9B** and **11B**, respectively. The structure of **11B** was determined by X-ray diffraction analysis. If thiophene is regarded as a sulfur-bridged butadiene, the behaviors exhibited upon the oxidation of **2** and **7** is very similar to those seen for bis(ruthenocenyl)butadienes.[12] The two-electron oxidized species **14** derived from **5** was also found to be stable but showed a temperature-dependent ^{1}H NMR spectrum in CD_3NO_2. This species exists as a fulvene complex-type structure (**14B**) at low temperature, but appears in a different form (**14A** or **14C**) at room temperature. Thus, the behavior of the electronic spins in the two-electron oxidized species of biruthenocenes bridged by thiophene derivatives, that is, the fate of the fulvene complex-type structure, seems to depend largely on the character of the thiophene derivatives, although no product has been detected that corresponds to the appearance of the triplet spins in the two-electron oxidized species of bis(ruthenocenyl)butadiynes.[13]

Experimental Section

General

All reactions were carried out under an atmosphere of N_2 and/or Ar and workups were performed without precaution to exclude air. NMR spectra were recorded with Bruker AC300P, AM400, or ARX400 spectrometers. Dry solvents were prepared by distillation from the appropriate drying agent prior to use as follows: CH_2Cl_2 (CaH_2), $ClCH_2CH_2Cl$ ($CaCl_2$), CH_3CN (CaH_2), benzene (Na), THF (Na-benzophenone), and DMF (CaH_2). 2-Ruthenocenyl-1,3-dioxaborolane (**1**),[14] 1,4-bis(ruthenocenyl)buta-1,3-diyne,[19] 1,4-bis(1′′,2′′,3′′,4′′,5′′-pentamethylruthenocenyl)buta-1,3-diyne,[13]

1,8-bis(1′′,2′′,3′′,4′′,5′′-pentamethylruthenocenyl)octa-1,3,5,7-tetrayne,[13] thieno[3,2-*b*]thiophene,[20] 3,6-dimethylthieno[3,2-*b*]-thiophene,[21] 2,5-diiodo-3,4-ethylenedioxythiophene,[22] dichloro-[1,1′-bis(diphenylphosphanyl)ferrocene]palladium, (dppf)$PdCl_2$,[23] and ferricenium tetra{3,5-bis(trifluoromethyl)phenyl}borate[24] were prepared according to the literature procedures. Other reagents were used as received from commercial suppliers.

Cyclic voltammetric and thin-layer coulometric measurements[16] were carried out with an ALS 400A Electrochemical Analyzer at 20 °C. A three-electrode cell containing of a glassy carbon disk working electrode (diameter 0.3 cm), Pt-coil counter electrode and an Ag/AgCl (3 M NaCl) reference electrode were employed. The ferrocene/ferrecenium (FcH/FcH^+) redox couple was used as an internal standard of the potential. Tetrabutylammonium tetrafluoroborate (nBu)$_4BF_4$ (Nacalai Tesque Inc.) was purified by recrystallization to be used as a supporting electrode. All solutions were degassed with high-purity argon prior to the electrochemical measurements.

2,5-Diiodo-thieno[3,2-*b*]thiophene: To a solution of thieno[3,2-*b*]-thiophene (0.11 g, 0.80 mmol) in dry benzene (10 mL) was slowly added iodine (0.43 g, 1.70 mmol) and HgO (0.17 g, 0.80 mmol) which were grinded together. The mixture was refluxed for 2 h and then cooled to room temp. After filtration, the residue was washed with CH_2Cl_2. The filtrate and the washings were combined, washed with a saturated solution of $Na_2S_2O_3$, and then dried with $MgSO_4$. After evaporation of the solvent, the residue was recrystallized from EtOH. Colorless crystals. Yield 0.20 g, 63%. M.p. 188–189 °C. ^{1}H NMR (300 MHz, $CDCl_3$): δ = 7.35 (s, 2 H, =CH) ppm. ^{13}C NMR (100 MHz, $CDCl_3$): δ = 75.6 (=C–I), 127.6 (=CH), 144.0 (=C) ppm. $C_6H_2I_2S_2$ (392.01): calcd. C 18.38, H 0.51; found C 18.56, H 0.44.

2,5-Diiodo-3,6-dimethylthieno[3,2-*b*]thiophene: This compound was prepared from 3,6-dimethylthieno[3,2-*b*]thiophene (0.21 g, 1.25 mmol) according to the procedure described above. Colorless crystals. Yield 0.30 g, 58%., M.p. >200 °C. ^{1}H NMR (300 MHz, $CDCl_3$): δ = 2.26 (s, 6 H, Me) ppm. ^{13}C NMR (100 MHz, $CDCl_3$): δ = 16.9 (Me), 99.7 (=C–I), 134.3 (=CH), 142.2 (=C) ppm. $C_8H_6I_2S_2$ (420.07): calcd. C 22.87, H 1.44; found C 23.13, H 1.35.

2,5-Bis(ruthenocenyl)thiophene (2): *Method A*: A mixture of 1,4-bis(ruthenocenyl)buta-1,3-diyne (0.102 g, 0.2 mmol) and NaSH (0.23 g, 4 mmol) in DMF (10 mL) was heated at 100 °C for 24 h under an atmosphere of Ar. After the reaction was cooled, H_2O (40 mL) was added to the solution, and the mixture was stirred for 0.5 h. The resulting crystals were collected by filtration under reduced pressure. The crystals were recrystallized from $CHCl_3$/hexane (2:1) to afford the title complex (97 mg, 87%) as yellow needles. M.p. 199–199.5 °C. ^{1}H NMR (400 MHz, $CDCl_3$): δ = 4.52 (s, 10 H), 4.60 (t, J = 1.9 Hz, 4 H), 4.94 (t, J = 1.9 Hz, 4 H), 6.69 (s, 2 H) ppm. ^{13}C NMR (100 MHz, $CDCl_3$): δ = 69.91 (η-C_5H_4), 70.44 (η-C_5H_4), 71.74 (η-C_5H_5), 84.22 (η-C_5H_4-*ipso*), 123.11 (=CH), 146.01 (=CS) ppm. $C_{24}H_{20}Ru_2S$ (542.63): calcd. C 53.12, H 3.72; found C 52.97, H 3.65.

Method B: 2,5-Diiodothiophene (0.12 g, 0.30 mmol), **1** (0.29 g, 1.6 mmol), (dppf)$PdCl_2$ (20 mg), DME (3 mL), and NaOH (10% aqueous solution, 3 mL) was sealed in an ample tube under an atmosphere of Ar. The ample tube was heated at 100 °C for 12 h. After the reaction was cooled to room temperature, the contents of the ampule were washed out with CH_2Cl_2, and the mixture was filtered. The organic layer was washed with water and then dried with Mg_2SO_4. After evaporation, the residue was dissolved in benzene, and the solution was then chromatographed on Al_2O_3 by elution with hexane/benzene to afford pale yellow crystals (42 mg, 23%). ^{1}H NMR (300 MHz, $CDCl_3$): δ = 4.52 (s, 10 H), 4.60 (t, J = 2 Hz, 4 H), 4.94 (t, J = 2 Hz, 4 H), 6.69 (s, 2 H) ppm. ^{13}C NMR (100 MHz, $CDCl_3$): δ = 69.91, 70.44, 71.74, 84.22, 123.11, 146.01 ppm.

2,5-Bis(ruthenocenyl)-3,4-ethylenedioxythiophene (3): This compound was prepared from 2,5-diiodo-3,4-ethylenedioxythiophene according to *Method B* described above. Yellow crystals. Yield 38%. M.p. 253–254 °C. ^{1}H NMR (400 MHz, $CDCl_3$): δ = 4.19 (s, 4 H, CH_2), 4.53 (s, 10 H, η-C_5H_5), 4.59 (t, J = 1.6 Hz, 4 H, η-C_5H_4), 5.00 (t, J = 1.6 Hz, 4 H, η-C_5H_4) ppm. ^{13}C NMR (100 MHz, $CDCl_3$): δ = 64.59 (CH_2), 69.95 (η-C_5H_4), 70.12 (η-C_5H_4), 71.44 (η-C_5H_5), 81.81 (*ipso*- η-C_5H_4), 111.52 (=C–S), 137.08 (=C–O) ppm. $C_{26}H_{22}O_2Ru_2S$ (660.66): calcd. C 51.99, H 3.69; found C 52.34, H 3.52.

5,5′-Bis(ruthenocenyl)-2,2′-bithiophene (4): This compound was prepared from 5,5′-diiodo-2,2′-bithiophene according to the procedure described above. Yellow crystals. Yield 23%. M.p. 253–254 °C. ^{1}H NMR (400 MHz, $CDCl_3$): δ = 4.53 (s, 10 H, η-C_5H_5), 4.63 (t, J = 1.8 Hz, 4 H, η-C_5H_4), 4.98 (t, J = 1.8 Hz, 4 H, η-C_5H_4), 6.82 (d, J = 3.8 Hz, 2 H, =CH), 6.86 (d, J = 3.8 Hz, 2 H, =CH) ppm. ^{13}C NMR (100 MHz, $CDCl_3$): δ = 69.86 (η-C_5H_4), 70.63 (η-C_5H_4), 71.88 (η-C_5H_5), 83.57 (*ipso*-η-C_5H_4), 122.94 (=CH), 123.79 (=CH), 135.08 (=C–S), 141.24 (=C–S) ppm. $C_{28}H_{22}Ru_2S_2$·1/4$CHCl_3$ (654.60): calcd. C 51.61, H 3.44; found C 51.50, H 3.35.

2,5-Bis(ruthenocenyl)thieno[3,2-*b*]thiophene (5): This compound was prepared from 2,5-diiodothieno[3,2-*b*]thiophene according to the procedure described above (reaction time: 2 h). Yellow crystals. Yield 18%. M.p. >250 °C. ^{1}H NMR (400 MHz, $CDCl_3$): δ = 4.53 (s, 10 H, η-C_5H_5), 4.64 (t, J = 1.8 Hz, 4 H, η-C_5H_4), 5.00 (t, J = 1.8 Hz, 4 H, η-C_5H_4), 7.00 (s, 2 H, =CH) ppm. ^{13}C NMR (100 MHz, $CDCl_3$): δ = 69.99 (η-C_5H_4), 70.62 (η-C_5H_4), 71.90 (η-C_5H_5), 115.27 (=CH) ppm. No quaternary carbon was observed because of its insolubility. $C_{26}H_{20}Ru_2S_2$ (598.71): calcd. C 52.16, H 3.37; found C 52.16, H 3.36.

2,5-Bis(ruthenocenyl)-3,6-dimethylthieno[3,2-*b*]thiophene (6): This compound was prepared from 2,5-diiodo-3,6-dimethylthieno[3,2-*b*]-thiophene according to the procedure described above (reaction time: 5 h). Yellow crystals. Yield 25%. M.p. >250 °C. ^{1}H NMR (400 MHz, $CDCl_3$): δ = 2.28 (s, 6 H, Me), 4.58 (s, 10 H, η-C_5H_5), 4.64 (t, J = 1.7 Hz, 4 H, η-C_5H_4), 4.93 (t, J = 1.7 Hz, 4 H, η-C_5H_4) ppm. ^{13}C NMR (100 MHz, $CDCl_3$): δ = 70.43 (η-C_5H_4), 71.73 (η-C_5H_5), 71.78 (η-C_5H_4), 84.66 (*ipso*-η-C_5H_4), 126.03 (=C–C), 135.44 (=C–S), 137.50 (=C–S) ppm. $C_{28}H_{24}Ru_2S_2$ (626.76): calcd. C 53.66, H 3.86; found C 53.48, H 3.56.

2,5-Bis(1′′,2′′,3′′,4′′,5′′-pentamethylruthenocenyl)thiophene (7): A mixture of 1,4-bis(1′′,2′′,3′′,4′′,5′′-pentamethylruthenocenyl)buta-1,3-diyne (97 mg, 0.15 mmol) and NaSH (84 mg, 1.5 mmol) in DMF (20 mL) was stirred and heated at 100 °C for 24 h under an atmosphere of Ar. After the reaction was cooled, the mixture was diluted with benzene (50 mL). The solution was washed twice with saturated aqueous LiCl and subsequently with H_2O and then dried with $MgSO_4$. After evaporation, the residue was chromatographed on Al_2O_3 (deactivated with 5% H_2O) and eluted with hexane/benzene (10:1) to afford the title complex (94 mg, 92%) as yellow solid. M.p. 243 °C. ^{1}H NMR (400 MHz, C_6D_6): δ = 1.81 (s, 15 H, Me), 4.23 (t, J = 1.7 Hz, 4 H, η-C_5H_4), 4.57 (t, J = 1.7 Hz, 4 H, η-C_5H_4) 6.66 (s, 2 H, =CH) ppm. ^{13}C NMR (100 MHz, C_6D_6): δ = 11.58 (Me), 70.86 (η-C_5H_4), 73.20 (η-C_5H_4), 84.36 (*ipso* -η-C_5H_4), 85.39 (η-C_5Me_5), 121.48 (=CH), 137.56 (=C–S) ppm. $C_{34}H_{40}Ru_2S$ (682.90): calcd. C 59.80, H 5.90; found C 59.69, H 5.86.

5,5′-Bis(1′′,2′′,3′′,4′′,5′′-pentamethylruthenocenyl)-2,2′-bithiophene (8): This compound was prepared from 1,8-bis(1′′,2′′,3′′,4′′,5′′-

pentamethylruthenocenyl)octa-1,3,5,7-tetrayne according to the procedure described above (reaction temperature: 110 °C). Red–orange solid. Yield 64%. M.p. 230 °C (dec.). ^{1}H NMR (400 MHz, $CDCl_3$): δ = 1.79 (s, 30 H, Me), 4.29 (t, J = 1.6 Hz, 4 H, η-C_5H_4), 4.53 (t, J = 1.6 Hz, 4 H, η-C_5H_4), 6.69 (d, J = 3.8 Hz, 2 H, =CH), 6.90 (d, J = 3.8 Hz, 2 H, =CH) ppm. ^{13}C NMR (100 MHz, $CDCl_3$): δ = 11.33 (Me), 70.64 (η-C_5H_4), 73.24 (η-C_5H_4), 82.96 (*ipso*-η-C_5H_4), 85.52 (η-C_5Me_5), 121.12 (=CH), 122.81 (=CH), 133.63 (=C–S), 140.07 (=C–S) ppm. $C_{38}H_{42}Ru_2S_2$ (765.02): calcd. C 59.66, H 5.53; found C 59.47, H 5.42.

Chemical Oxidation of Complex 2: To a solution of **2** (16.3 mg, 0.03 mmol) and *p*-BQ (6.3 mg, 0.06 mmol) in $CHCl_3$ (3 mL) chilled at 0 °C by an ice bath was added BF_3·OEt_2 (2 drops from a capillary) under an atmosphere of nitrogen. After the resulting dark brown solution had been stirred for 5 min at 0 °C, dry benzene (3 mL) was added to the solution and then kept for 30 min at the same temperature. The mixture was filtered under reduced pressure and washed with pentane to afford a black powder (16 mg) (The product contained hydroquinone). ^{1}H NMR (400 MHz, CD_3NO_2, 0 °C): δ = 5.26 (s, 10 H), 5.75 (br. s, 2 H), 5.90 (br. s, 2 H), 6.32 (br. s, 2 H), 6.40 (br. s, 2 H), 7.46 (s, 2 H) ppm. ^{1}H NMR (400 MHz, CD_3CN, –5 °C): δ = 4.57 (s, 5 H, η-C_5H_5), 5.02 (t, J = 1.8 Hz, 2 H, η-C_5H_4), 5.36 (t, J = 1.8 Hz, 2 H, η-C_5H_4), 5.88 (s, 5 H, η-C_5H_5), 6.01 (t, J = 2.6 Hz, 2 H, η-C_5H_4), 6.27 (t, J = 2.6 Hz, 2 H, η-C_5H_4), 7.40 (d, J = 4.5 Hz, 1 H, =CH), 8.05 (d, J = 4.5 Hz, 1 H, =CH) ppm. ^{13}C NMR (100 MHz, CD_3NO_2, –5 °C): δ = 77.42 (η-C_5H_4), 78.72 (η-C_5H_4), 86.24 (η-C_5H_5), 90.33 (η-C_5H_4), 90.66 (η-C_5H_4), 92.90 (*ipso*-η-C_5H_4), 129.96 (=C–S), 137.01 (=CH) ppm.

Chemical Oxidation of Complex 7: *Method A*: To a solution of **7** (20.5 mg, 0.03 mmol) and *p*-BQ (6.3 mg, 0.06 mmol) in dry CH_2Cl_2 (3 mL) chilled at 0 °C by an ice bath was added BF_3·OEt_2 (1 drop from a capillary) under an atmosphere of nitrogen. After the resulting red–violet solution had been stirred for 3 min at 0 °C, dry benzene (6 mL) was added to the solution, and the stirring was then stopped. After the solution had been kept for 30 min at 0 °C, dry benzene (9 mL) was added to the solution, and the solution was then kept for 1 h at the same temperature. The mixture was filtered under reduced pressure and washed with pentane to afford black powdery crystals (16 mg) (The product contained hydroquinone). The crystals were comparably stable when stored in the freezer. The solution of the product in CD_3NO_2 or CD_3CN immediately after its preparation produced a clear ^{1}H NMR spectrum. ^{1}H NMR (400 MHz, CD_3NO_2, –5 °C): δ = 1.79 (s, 30 H), 5.53 (t, J = 2.0 Hz, 4 H), 5.90 (m, 4 H), 7.41 (s, 2 H) ppm. ^{1}H NMR (400 MHz, CD_3CN, 0 °C): δ = 1.66 (s, 15 H), 1.92 (s, 15 H), 4.78 (t, J = 1.8 Hz, 2 H), 4.94 (br. s, 2 H), 5.57 (t, J = 2.3 Hz, 2 H), 5.69 (m, 2 H), 7.11 (d, J = 4.6 Hz, 1 H), 7.99 (d, J = 4.6 Hz, 1 H) ppm. ^{13}C NMR (100 MHz, CD_3NO_2, –5 °C): δ = 7.39 (Me), 75.85 (η-C_5H_4), 77.10 (η-C_5H_4), 93.81 (η-C_5H_4), 93.99 (η-C_5H_4), 95.34 (*ipso*-η-C_5H_4), 98.49 (η-C_5Me_5), 132.93 (=C–S), 136.58 (=CH) ppm.

Method B: To a solution of **7** (13.7 mg, 0.02 mmol) in dry CH_2Cl_2 (3 mL) was added ferricenium tetra{3,5-bis(trifluoromethyl)-phenyl}borate (42 mg, 0.04 mmol) at 0 °C under an atmosphere of nitrogen. After the resulting red–violet solution had been stirred for 15 min at 0 °C, dry benzene (6 mL) was added to the solution and the stirring was then stopped. After the solution had been kept for 30 min at 0 °C, dry benzene (9 mL) was added to the solution, and the solution was then kept for 1.5 h at the same temperature. The resulting fine crystals were collected by filtration under reduced pressure. Dark red–violet fine crystals (37 mg). ^{1}H NMR (400 MHz, CD_2Cl_2, 0 °C): δ = 1.70 (s, 30 H, Me), 5.19 (m, 2 H, η-C_5H_4), 5.24 (m, 2 H, η-C_5H_4), 5.65 (t, J = 2.1 Hz, 4 H, η-C_5H_4), 7.02 (s, 2 H, =CH), 7.56 (br. s, 8 H, C_6H_3), 7.72 (br. s, 16 H, C_6H_3) ppm. ^{1}H NMR (400 MHz, [D$_6$]acetone, 0 °C): δ = 1.83 (s, 30 H, Me), 5.81 (br. s, 2 H, η-C_5H_4), 5.89 (br. s, 2 H, η-C_5H_4), 6.17 (br. s, 4 H, η-C_5H_4), 7.68 (br. s, 8 H, C_6H_3), 7.77 (br. s, 16 H, C_6H_3), 7.83 (s, 2 H, =CH) ppm. ^{1}H NMR (400 MHz, CD_3NO_2, 0 °C): δ = 1.80 (s, 30 H, Me), 5.52 (m, 4 H, η-C_5H_4), 5.90 (m, 4 H, η-C_5H_4), 7.41 (s, 2 H, =CH), 7.67 (br. s, 8 H, C_6H_3), 7.84 (br. s, 16 H, C_6H_3) ppm. ^{1}H NMR (400 MHz, CD_3CN, –10 °C): δ = 1.65 (s, 15 H, Me), 1.91 (s, 15 H, Me), 4.78 (t, J = 1.8 Hz, 2 H, η-C_5H_4), 4.93 (m, 2 H, η-C_5H_4), 5.56 (t, J = 2.4 Hz, 4 H, η-C_5H_4), 5.67 (m, 2 H, η-C_5H_4), 7.10 (d, J = 4.6 Hz, 1 H, =CH), 7.35 (br. s, 8 H, C_6H_3), 7.67 (br. s, 16 H, C_6H_3), 7.98 (d, J = 4.6 Hz, 1 H, =CH) ppm. $C_{98}H_{64}B_2F_{48}Ru_2S$ (2409.35): calcd. C 48.85, H 2.68; found C 48.42, H 2.61.

Chemical Oxidation of Complex 5: To a solution of **5** (8.0 mg, 0.015 mmol) and *p*-BQ (3.2 mg, 0.03 mmol) in $CHCl_3$ (3 mL) chilled at 0 °C by an ice bath was added BF_3·OEt_2 (2 drops from a capillary) under an atmosphere of nitrogen. After the resulting dark brown solution had been stirred for 1 h at 0 °C, dry Et_2O (6 mL) was added to the solution and the stirring was then stopped. The solution was kept for 1 h at the same temperature. The reaction was filtered under reduced pressure and washed with pentane to afford black crystals (6.5 mg) that were stable when stored in the freezer. The solution of the product in CD_3NO_2 (deep blue–violet) or CD_3CN (deep blue) produced a clear ^{1}H NMR spectrum. ^{1}H NMR (400 MHz, CD_3NO_2, 20 °C): δ = 5.27 (s, 10 H), 5.93 (t, J = 1.9 Hz, 4 H), 6.30 (t, J = 1.9 Hz, 4 H), 7.53 (s, 2 H) ppm. ^{13}C NMR (100 MHz, CD_3NO_2, 20 °C): δ = 76.50 (η-C_5H_4), 84.18 (η-C_5H_5), 88.79 (η-C_5H_4), 95.77 (*ipso*- η-C_5H_4), 125.88 (=CH) ppm. ^{1}H NMR (400 MHz, CD_3NO_2, –35 °C): δ = 5.24 (s, 10 H), 5.88 (br. s, 2 H), 5.98 (br. s, 2 H), 6.27 (br. s, 4 H), 7.51 (s, 2 H) ppm. ^{1}H NMR (400 MHz, CD_3CN, 0 °C): δ = 4.55 (s, 5 H), 4.93 (br. s, 2 H), 5.29 (br. s, 2 H), 5.90 (s, 5 H), 6.12 (br. s, 5 H), 6.34 (br. s, 2 H), 7.45 (s, 1 H), 8.32 (s, 1 H) ppm.

Electronic Structure Calculation

DFT calculations were performed with the Gaussian 03 package program.[25] The calculation at the B3LYP hybrid density-functional levels[26,27] with the 3-21G basis set did not reproduce the optimized structure of the two-electron oxidized species in the present series determined by the NMR spectra and X-ray analysis. In order to understand this source, extensive DFT calculations for ruthenocene ($C_{10}H_{10}Ru$ with D_{5h} symmetry) have also been performed with various combinations of exchange and correlation functionals. As a result, we have chosen to use the local spin density approximation (LSDA) with the Vosko–Wilk–Nusair exchange-correlation potential[28] for the calculation of our systems, because the previous theoretical study[29,30] at this level for ruthenocene showed relatively good agreement with the experimental data and give the order of $3e'_2 < 5a'_1 < 4e''_1$ [$(3e'_2)^4(5a'_1)^2(4e''_1)^0$]. Notice that the HOMO of ruthenocene is an a_{1g} orbital and this gives a significant result in the ionization state of ruthenocene and the structure of the dications of binuclear ruthenocene derivatives. Thus, it may be suggested that the extraction of an electron from the a_{1g} orbital of the ruthenocene moiety of **2** and **7** is likely to cause the deformation of the bridging ligand in **10** and **12**, respectively.

A Stuttgart–Dresden–Bonn quasirelativistic ECP28 MWB (SDD) effective core potential[31] have been employed for ruthenium atoms. The standard 6-311G basis sets were used for C and H atoms, whereas the 6-311G(*d*) basis set was used to describe the

Table 5. Crystallographic data for **3**, **7**, and **13**.

	3	**7**	**13**
Empirical formula	$C_{26}H_{22}O_2Ru_2S$	$C_{34}H_{40}Ru_2S$	$C_{106}H_{84}B_2F_{48}O_2Ru_2S$
Formula mass	600.664	682.898	2557.55
Crystal system	Monoclinic	Triclinic	Triclinic
Space group	$P21/c$	$P\bar{1}$	$P\bar{1}$
a [Å]	11.8770(10)	7.8370(8)	14.0768(7)
b [Å]	14.3180(10)	13.5590(13)	14.4758(7)
c [Å]	12.7840(10)	15.458(2)	15.5151(8)
α [°]	90	105.672(6)	88.9260(10)
β [°]	92.372(7)	102.038(5)	76.1620(10)
γ [°]	90	99.768(10)	63.8540(10)
V [Å^3]	2172.1(3)	1501.5(3)	2742.0(2)
Z	4	2	1
$D_{calcd.}$ [Mg m^{-3}]	1.837	1.510	1.549
Crystal size [mm]	0.20 × 0.15 × 0.08	0.18 × 0.06 × 0.02	0.28 × 0.14 × 0.12
Radiation (λ [Å])	Mo-K_α (0.71073)	Mo-K_α (0.71073)	Mo-K_α (0.71073)
Reflection (hkl) limits	$-15 \le h \le 15$	$-9 \le h \le 9$	$-18 \le h \le 17$
	$0 \le k \le 18$	$-15 \le k \le 15$	$-19 \le k \le 15$
	$0 \le l \le 15$	$0 \le l \le 19$	$-17 \le l \le 20$
Total reflections measured	4466	5203	20164
Unique reflections	4314	5198	12980
Linear abs. coeff. [mm^{-1}]	1.508	1.10	0.424
Reflections used in L.S.	4314	5198	12980
R	0.0688	0.0681	0.0789
Rw	0.1886	0.1881	0.2131
S	1.087	1.035	0.997
Max peak in final Fourier map [e Å^{-3}]	0.792	0.861	1.092
Min peak in final Fourier map [e Å^{-3}]	–1.432	–0.922	–0.788

hypervalency of the sulfur atom. In order to further examine the effect of polarization, larger basis sets of 6-311G(*d*) have also been employed for C and H and 6-311G(2*d*) for S.

Structure Determination

The crystallographic data are listed in Table 5 for **3**, **7**, and **13**. Data collection of crystal data for **3** and **7** was performed at room temperature with a Mac Science DIP3000 image processor. The structures of **3** and **7** were solved with the Dirdif-Patty method in MAXUS (software package for structure determination) and refined finally by full-matrix least-squares procedure with SHELEX. Crystal data for **13** were collected at –196 °C (liquid N_2) with a Bruker Apex diffractometer with graphite monochromated Mo-K_α radiation and an 18-kW rotating anode generator. The structure of **13** was solved and refined by SHELEX. Absorption correction for **3** and **7** was carried out by the Sortav method and anisotropic refinement for non-hydrogen atom was carried out. The hydrogen atoms, located from difference Fourier maps or calculation, were isotropically refined.

CCDC-298964 (**3**), -298965 (**7**), and -298966 (**13**) contain the supplementary crystallographic data for this paper. These data can be obtained free of charge from The Cambridge Crystallographic Data Centre via www.ccdc.cam.ac.uk/data_request/cif..

[1] a) M. D. Ward, *Chem. Soc. Rev.* **1995**, *24*, 121–134; b) V. Grosshenny, A. Harriman, R. Ziessel, *Angew. Chem. Int. Ed. Engl.* **1995**, *34*, 1100–1102.

[2] a) M. Altmann, U. F. H. Bunz, *Angew. Chem. Int. Ed. Engl.* **1995**, *34*, 569–571; b) L. Oriol, J. L. Serrano, *Adv. Mater.* **1995**, *7*, 348–369.

[3] J.-M. Lehn, *Suppramolecular Chemistry: Concepts and Perspectives*, VCH Publishers, Weinheim, Germany, **1995**.

[4] M. I. Bruce, P. J. Low, *Adv. Organomet. Chem.* **2004**, *50*, 179–444.

[5] a) F. Paul, C. Lapinte, *Coord. Chem. Rev.* **1998**, *178–180*, 431–509; b) U. H. Bunz, *Angew. Chem. Int. Ed. Engl.* **1996**, *35*, 969–971; c) A. Nakamura, *Bull. Chem. Soc. Jpn.* **1995**, *68*, 1515–1521; d) N. J. Long, *Angew. Chem. Int. Ed. Engl.* **1995**, *34*, 21–38; e) H. Lang, *Angew. Chem. Int. Ed. Engl.* **1994**, *33*, 547–550; f) W. Beck, B. Niemer, M. Wieser, *Angew. Chem. Int. Ed. Engl.* **1993**, *32*, 923–949.

[6] D. Astruc, *Electron Transfer and Radical Process in Transition-Metal Chemistry*, VCH, New York, **1995**.

[7] a) G.-L. Xu, R. J. Crutchley, M. C. DeRosa, Q.-J. Pan, H.-X. Zhang, X. Wang, T. Ren, *J. Am. Chem. Soc.* **2005**, *127*, 13354–13363; b) W. Skibar, H. Kopacka, K. Wurst, C. Salzmann, K.-H. Ongania, F. Fabrizi de Biani, P. Zanello, B. Bildstein, *Organometallics* **2004**, *23*, 1024–1041; c) J. H. K. Yip, J. Wu, K.-Y. Wong, K. P. Ho, C. S.-N. Pun, J. J. Vittal, *Organometallics* **2002**, *21*, 5292–5300; d) N. J. Long, *Metallocens: An Introduction to Sandwich Complexes*, Blackwell Science, Oxford, UK, **1998**; e) A. Hradsky, B. Bildstein, N. Schuler, H. Schottenberger, P. Jaitner, K.-H. Ongania, K. Wurst, J.-P. Laumay, *Organometallics* **1997**, *16*, 392–402; f) N. D. Jones, M. O. Wolf, D. M. Giaquinta, *Organometallics* **1997**,*16*, 1352–1354; g) M. C. B. Colbert, J. Lewis, N. J. Long, P. R. Raithby, A. J. P. White, D. J. Williams, *J. Chem. Soc., Dalton Trans.* **1997**, 99–104; h) A.-C. Ribou, J.-P. Launay, M. L. Sachtleben, H. Li, C. W. Spangler, *Inorg. Chem.* **1996**, *35*, 3735–3740; i) Z. Yuan, G. Stringer, I. R. Jobe, D. Kreller, L. Koch, N. J. Taylor, T. B. Marder, *J. Organomet. Chem.* **1993**, *452*, 115–120.

[8] a) S.-M. Lee, M. Marcaccio, J. A. McCleverty, M. D. Ward, *Chem. Mater.* **1998**, *10*, 3272–3274; b) R. D. McCullough, *Adv. Mater.* **1998**, *10*, 93–116; c) J. Roncali, *Chem. Rev.* **1997**, *97*, 173–205; d) J. M. Tour, *Chem. Rev.* **1996**, *96*, 537–553; e) M. C. B. Colbert, D. Hodgson, J. Lewis, P. R. Raithby, N. J. Long, *Polyhedron* **1995**, *14*, 2759–2766.

[9] a) P. Li, B. Ahrens, H. Feeder, P. R. Raithby, S. T. Teat, M. S. Khan, *Dalton Trans.* **2005**, 874–883; b) M. Landman, H. Görls, S. Lotz, *Eur. J. Inorg. Chem.* **2001**, 233–238; c) R. D. A. Hudson, A. R. Manning, D. F. Nolan, I. Asselberghs, R. V. Boxe-

151l, A. Persoons, J. F. Gallagher, *J. Organomet. Chem.* **2001**, *619*, 141; d) S. L. Stang, F. Paul, C. Lapinte, *Organometallics* **2000**, *19*, 1035–1043; e) M. C. B. Colbert, J. Lewis, N. J. Long, P. R. Raithby, M. Younus, A. J. P. White, D. J. Williams, N. N. Payne, L. Yellowlees, D. Beljonne, N. Chawdhury, R. H. Friend, *Organometallics* **1998**, *17*, 3034–3043; f) J. Lewis, N. J. Long, P. R. Raithby, G. P. Shields, W.-Y. Wong, M. Younus, *J. Chem. Soc. Dalton Trans.* **1997**, 4283–4288.

[10] a) B. Jacques, J.-P. Tranchier, F. Rose-Munch, E. Rose, *Organometallics* **2004**, *23*, 184–193; b) W.-Y. Wong, G.-L. Lu, A.-F. Ng, K.-H. Choi, Z. Lin, *J. Chem. Soc. Dalton Trans.* **2001**, 3250–3260; c) Y. Zhu, M. O. Wolf, *J. Am. Chem. Soc.* **2000**, *122*, 10121–10125; d) K. R. Justin Thomas, J. T. Lin, Y. S. Wen, *Organometallics* **2000**, *19*, 1008–1012; e) M. Sato, M. Shiraogawa, *CACS Forum* **1993**, *13*, 30–32.

[11] M. Watanabe, M. Sato, T. Takayama, *Organometallics* **1999**, *18*, 5201–5203.

[12] a) M. Sato, T. Nagata, A. Tanemura, T. Fujihara, S. Kumakura, K. Unoura, *Chem. Eur. J.* **2004**, *10*, 2166–2178; b) M. Sato, Y. Kawata, A. Kudo, A. Iwai, H. Saitoh, S. Ochiai, *J. Chem. Soc. Dalton Trans.* **1998**, 2215–2224; c) M. Sato, A. Kudo, Y. Kawata, H. Saitoh, *Chem. Commun.* **1996**, 25–26.

[13] a) M. Sato, Y. Kubota, Y. Kawata, T. Fujihara, K. Unoura, A. Oyama, *Chem. Eur. J.* **2006**, *12*, 2282–2292; b) M. Sato, M. Watanabe, *Chem. Commun.* **2002**, 1574–1575.

[14] M. Sato, G. Maruyama, A. Tanemura, *J. Organomet. Chem.* **2002**, *655*, 23–30.

[15] D. Obendorf, H. Schottenberger, K. Wurst, N. Schuler, G. Laus, *J. Organomet. Chem.* **2005**, *690*, 811–817.

[16] K. Unoura, A. Iwase, H. Ogino, *J. Electro. Chem. Interfacial Electrochem.* **1990**, *295*, 385–392.

[17] S. Barlow, A. Cowley, J. C. Green, T. J. Brunker, T. Hascall, *Organometallics* **2001**, *20*, 5351–5359.

[18] A. I. Yanovsky, Yu. T. Struchkov, A. Z. Kleindlin, M. I. Rybinskaya, *J. Organomet. Chem.* **1989**, *369*, 125–130.

[19] O. Hofer, K. Schlögl, *J. Organomet. Chem.* **1968**, *13*, 443–456.

[20] L. S. Fuller, B. Iddon, K. A. Smith, *J. Chem. Soc. Perkin Trans. 1* **1977**, 3465–3470.

[21] K. S. Choi, K. Sawada, H. Dong, M. Hoshino, J. Nakayama, *Heterocycles* **1994**, *38*, 143–149.

[22] H. Meng, D. F. Perepichka, M. Bendikov, F. Wudl, G. Z. Pan, W. Yu, W. Dong, B. Brown, *J. Am. Chem. Soc.* **2003**, *125*, 15151–15162.

[23] T. Hayashi, M. Konishi, Y. Kobori, M. Kumada, T. Higuchi, K. Hirotsu, *J. Am. Chem. Soc.* **1984**, *106*, 158–163.

[24] I. Chávez, A. Alverez-Carena, E. Molins, A. Roig, W. Maniu-Kiewicz, A. Arancibia, V. Arencibia, H. Brand, I. M. Manríquez, *J. Organomet. Chem.* **2000**, *601*, 126–132.

[25] M. J. Frisch, G. W. Trucks, H. B. Schlegel, G. E. Scuseria, M. A. Robb, J. R. Cheeseman, J. A. Montgomery Jr, T. Vreven, K. N. Kudin, J. C. Burant, J. M. Millam, S. S. Iyengar, J. Tomasi, V. Barone, B. Mennucci, M. Cossi, G. Scalmani, N. Rega, G. A. Petersson, H. Nakatsuji, M. Hada, M. Ehara, K. Toyota, R. Fukuda, J. Hasegawa, M. Ishida, T. Nakajima, Y. Honda, O. Kitao, H. Nakai, M. Klene, X. Li, J. E. Knox, H. P. Hratchian, J. B. Cross, C. Adamo, J. Jaramillo, R. Gomperts, R. E. Stratmann, O. J. Yazyev, A. Austin, R. Cammi, C. Pomelli, J. W. Ochterski, P. Y. Ayala, K. Morokuma, G. A. Voth, P. Salvador, J. J. Dannenberg, V. G. Zakrzewski, S. Dapprich, A. D. Daniels, M. C. Strain, O. Farkas, D. K. Malick, A. D. Rabuck, K. Raghavachari, J. B. Foresman, J. V. Ortiz, Q. Cui, A. G. Baboul, S. Clifford, J. Cioslowski, B. B. Stefanov, G. Liu, A. Liashenko, P. Piskorz, I. Komaromi, R. L. Martin, D. J. Fox, T. Keith, M. A. Al-Laham, C. Y. Peng, A. Nanayakkara, M. Challacombe, P. M. W. Gill, B. Johnson, W. Chen, M. W. Wong, C. Gonzalez, J. A. Pople, *Gaussian 03*, Revision C.02, Gaussian, Inc., Wallingford, CT, **2004**.

[26] A. D. Becke, *J. Chem. Phys.* **1993**, *98*, 5648–5652.

[27] C. Lee, W. Yang, R. G. Parr, *Phys. Rev. B* **1988**, *37*, 785–789.

[28] S. H. Vosko, L. Wilk, N. Nusair, *Can. J. Phys.* **1980**, *58*, 1200–1211.

[29] C. Daul, H.-U. Güdel, J. Weber, *J. Chem. Phys.* **1993**, *98*, 4023–4029.

[30] F. Gilardoni, J. Weber, A. Hauser, C. Daul, *J. Chem. Phys.* **1998**, *109*, 1425–1434.

[31] A. Bergner, M. Dolg, W. Kuechle, H. Stoll, H. Preuss, *Mol. Phys.* **1993**, *80*, 1431–1441.

Received: April 26, 2006
Published Online: September 18, 2006

